Frequency Dependence of Sonophoresis

Ahmet Tezel,[1] Ashley Sens,[3] Joe Tuchscherer,[2] and Samir Mitragotri[1,4]

Received May 4, 2001; accepted August 31, 2001

Purpose. Application of low-frequency ultrasound has been shown to increase skin permeability, thereby facilitating delivery of macromolecules (low-frequency sonophoresis). In this study, we sought to determine the dependence of low-frequency sonophoresis on ultrasound frequency, intensity and energy density.

Methods. Pig skin was exposed to low-frequency ultrasound over a range of ultrasound frequency and intensity conditions. The degree of skin permeabilization was measured using its conductivity. Imaging experiments were also carried out to visualize the transport pathways created by ultrasound.

Results. The data showed that for each frequency (in the range of 19.6–93.4 kHz), there exists a threshold intensity below which no detectable conductivity enhancement was observed. The threshold intensity increased with frequency. It is feasible to achieve the desired conductivity (permeability) enhancement regardless of the choice of frequency, although the necessary energy density is higher at higher frequencies. Low frequencies (~20 kHz) induced localized transport compared to a more dispersed effect seen with higher frequencies (~58.9 kHz).

Conclusions. This study provides a quantitative understanding of the effects of low-frequency ultrasound on skin permeability.

KEY WORDS: cavitation; energy density; transdermal; sonophoresis; surfactant.

INTRODUCTION

Transdermal drug delivery (TDD) offers an advantageous alternative to common delivery methods such as injections or oral delivery. However, the applications of transdermal delivery are limited by low skin permeability. Specifically, stratum corneum (SC), the outermost layer of the skin, provides an outstanding barrier against the external environment and is responsible for skin's barrier properties (1–3). SC is a relatively thin (10–15 μm) impermeable membrane that consists of flat, dead cells, which are filled with keratin fibers (keratinocytes) that are surrounded by lipid bilayers (3,4). The highly ordered structure of lipid bilayers confers on the SC an impermeable character. Different techniques, such as chemical enhancers (3,5,6), iontophoresis (7), electroporation (8), ultrasound (sonophoresis) applied at both therapeutic (9) (1–3 MHz) and low-frequency (10) (20–100 kHz) conditions have been used to enhance transdermal drug transport.

Low-frequency ultrasound (f~20 kHz) is significantly more potent in enhancing skin permeability compared to therapeutic ultrasound (f~1–3 MHz) (11). This is a direct consequence of reduced acoustic cavitation (formation, growth, and collapse of gas bubbles) at high ultrasound frequencies (12). Application of ultrasound generates oscillating pressures in liquids and nucleates cavitation bubbles. At higher frequencies it becomes increasingly difficult to generate cavitation due to the fact that the time between the positive and negative acoustic pressures becomes too short, diminishing the ability of dissolved gas within the medium to diffuse into the cavitation nuclei.

Although the number and size of cavitation bubbles is inversely correlated with application frequency, a detailed dependence of ultrasonic transport enhancement on frequency in the low-frequency regime is still not known. Developing knowledge of this dependence is of fundamental as well as practical interest. Specifically, an in depth knowledge of the dependence of transport enhancement on ultrasound frequency and intensity should provide insight into the mechanisms of low-frequency sonophoresis. In addition, this knowledge should form a solid background for optimization and future studies for sonophoresis. The objective of this study is to develop this knowledge.

MATERIALS AND METHODS

In Vitro Experiments

In vitro experiments were carried out with full-thickness pig skin (Yorkshire). The animal was euthanized using pentobarbital (100 mg/kg). Skin on the back and the lateral flank was harvested immediately after sacrificing the animal. The underlying fat was removed and the skin, i.e., dermis and epidermis, was cut into small pieces (2.5 cm × 15 cm). Skin pieces with no visible imperfections such as scratches and abrasions were wrapped in aluminum foil and stored in a −80°C freezer to be used over a period of 12 weeks. Before each experiment the skin was thawed at room temperature and was mounted on to a Franz diffusion cell (Permegear, Hellertown, PA). Only skin having an initial resistivity of 30 kΩ-cm^2 or more was used to ensure that the skin was intact. Methods for conductivity measurement are described later.

A Franz diffusion cell consists of a donor and a receiver compartment. A 4-mm Ag/AgCl disk electrode (Invivo Metrics, Healdsburg, CA) was introduced in both compartments for skin conductivity measurements during the experiment. The receiver compartment was filled with a sodium/potassium phosphate buffered saline (PBS) (Sigma-Aldrich, St. Louis, MO). The solution has a phosphate concentration of 0.01 M and NaCl concentration of 0.137 M. PBS was prepared using deionized water with ~8 MΩ-cm resistivity. A magnetic stirrer bar was added to the receiver compartment. The donor compartment was filled with a solution of Sodium Lauryl Sulfate (SLS), (1% weight/volume) in PBS. SLS (Sigma-Aldrich, St. Louis, MO) was chosen as a model surfactant as its effect on transdermal transport in the presence of ultrasound has been relatively well-characterized (13). The diffusion cell was placed in a custom-made plexi-glass mounting block. The so-

[1] Department of Chemical Engineering, University of California Santa Barbara, Santa Barbara, California 93106.
[2] Department of Molecular, Cellular, Developmental Biology, University of California Santa Barbara, Santa Barbara, California 93106.
[3] Department of Chemistry, Santa Barbara City College, Santa Barbara, California 93109.
[4] To whom correspondence should be addressed. (E-mail: samir@engineering.ucsb.edu)

0724-8741/01/1200-1694/0 © 2001 Plenum Publishing Corporation

lution in the receiver compartment was stirred with a magnetic stirrer (Bell Stir, Vineland, NJ). Ultrasound was applied using the methods that will be described in the next section. All experiments were carried out at room temperature.

Ultrasound Application

Five custom built transducers with operating frequencies of 19.6, 36.9, 58.9, 76.6, and 93.4 kHz (Piezo Systems, Cambridge, MA) were used for application of ultrasound. The transducers were designed by sandwiching ceramic crystals between two metal resonators of appropriate length (6.1 cm, 2.9 cm, 6.1 cm, 4.6 cm, 3.6 cm respectively for 19.6 kHz, 36.9 kHz, 58.9 kHz, 76.6 kHz, and 93.4 kHz). The cross sectional area of all transducers was 0.785 cm^2. A signal generator (Tektronix CFG-280, Beaverton, OR) along with an amplifier (Krohn-Hite 7500, Avon, MA) was used to drive the transducers. The electric power applied to the transducer was measured using a sampling wattmeter (Clarke-Hess 2330, New York, NY). The frequency of the electrical signal was matched with the resonant frequency of each transducer. An inductor was connected in parallel with each transducer to optimize its performance. The values of the inductors were 1.06 H, 2980 mH, 1230 mH, 682 mH, 472 mH respectively for 19.6 kHz, 36.9 kHz, 58.9 kHz, 76.6 kHz, and 93.4 kHz. The transducer was placed at a distance of 3 mm from the skin in the donor compartment. A 100% duty cycle was chosen for ultrasound application as we have previously shown that the effect of duty cycle is insignificant. Each skin was sonicated in the presence of SLS. The ultrasonic intensity was measured with two independent systems, a laser interferometer (Polytec, Waldbronn, Germany) and a hydrophone (Reson, Goleta, CA). The intensity measurement procedures will be discussed in the next section. A typical temperature increase of <10°C, was observed in 2 min when ultrasound was applied. For this reason, the donor solution, i.e., coupling medium, was changed every 2 min during the experiment by turning off the ultrasound. Control experiments were carried out to assess the effect temperature on skin conductivity. No significant enhancement of skin conductivity was observed when the skin temperature was increased/decreased by 10°C without ultrasound.

Ultrasound Intensity Measurements

The power delivered by the sonicators could, in theory, be calculated by reading the wattage on the digital display of the wattmeter that is already integrated into the experimental setup. The power reading could then be converted to intensity by dividing the power with the transducer tip area. However, this calculation assumes that the sonicators are operating at 100% efficiency, an assumption that cannot be validated. The acoustic intensity of ultrasound is more relevant for sonophoresis rather than the electrical intensity measured by the wattmeter. For this reason, by two independent setups, we measured the pressure amplitude and the velocity amplitude of the transducer tip and then calculated the acoustic intensity, I, which is related to the motion of the transducer by the following equations:

$$I = v^2 \rho c \quad [1]$$

$$I = \frac{p^2}{pc} \quad [2]$$

where, p is the RMS pressure amplitude of the acoustic wave generated by the transducer, v is RMS velocity of amplitude transducer surface, p is water density (1000 kg/m^3), and c is speed of sound in water (1500 m/s). Thus, two independent estimates of the acoustic intensities were obtained, which allowed us to calculate the conversion efficiencies of each transducer. The velocity amplitude was measured by a laser interferometer and the pressure amplitude was measured using a hydrophone. These measurements are discussed next.

Laser Interferometer Measurements

A laser interferometer measures the velocity of a reflective surface (such as a transducer) based on optical interference. For this purpose, the donor compartment of a diffusion cell was mounted on a flat glass slide; giving a flat clear surface for the laser beam to enter the donor compartment with a 90° angle to the transducer tip. The donor compartment was filled with PBS or 1% SLS. The laser beam was aligned with the transducer and the beam was focused on the transducer surface. The interferometer was operated at a velocity calibration of 1000 mm/s/V. The output of the interferometer was analyzed with a dynamic signal analyzer code (National Instruments LabVIEW®, Austin, TX) through a data acquisition board (National Instruments 6052E, Austin, TX) connected to a PC. The output from the laser interferometer shows the existence of various frequency modes due to the presence of harmonics of the transducer oscillations. The component corresponding to the resonant frequency of the transducer was identified and the amplitude of the transducer velocity at this frequency was recorded. Acoustic intensity was calculated using this velocity based on Eq. 1. The transducer was activated at various electrical input powers and the velocity was recorded under these conditions. A direct correlation between the velocity and electrical power input (wattmeter measurements) was observed until the cavitation threshold was reached, after which accuracy of the measurements was compromised due to the scattering of the laser by cavitation bubbles.

Hydrophone Measurements

Pressure amplitude of the ultrasound wave was measured using a calibrated hydrophone. The hydrophone was placed ~1 mm perpendicular to the transducer tip surface in custom build polycarbonate chamber with a diameter equal to a donor compartment, i.e., 15 mm, of a diffusion cell. The chamber was filled with PBS or 1% SLS. No difference in measured intensities was observed when the chamber was filled with PBS or 1% SLS. Hence, PBS was used in the majority of experiments for simplicity. The output of the hydrophone was analyzed using a dynamic signal analyzer (Hewlett-Packard 3562A, Everett, WA) to capture the power spectrum of ultrasound. As in the case of laser interferometer measurements, various frequency components were observed in the acoustic spectrum obtained from the hydrophone. The signal corresponding to the resonant frequency of the transducer was identified and its magnitude was measured. RMS pressure amplitude of the ultrasound wave was then calculated using the calibration curve for the hydrophone that was pro-

vided by the manufacturer. Ultrasound intensity was calculated using Eq. 2. The hydrophone measurements were carried out at the same electrical intensities as the interferometer measurements to facilitate an accurate comparison.

The acoustic intensities measured by the laser interferometer and the hydrophone measurements agreed within 10%. The electrical-to-acoustic efficiency of the transducer was calculated using these measurements. All transducers were about 60% efficient (19.6 kHz – 69.2%, 36.9 kHz – 58.6%, 58.9 kHz – 63%, 76.6 kHz – 69.9%, 93.4 kHz – 67%). No systematic dependence of transducer efficiency on ultrasound frequency/intensity was observed. Accordingly, a single representative value for efficiency was used. To measure the acoustic intensity beyond cavitation threshold, we assumed that the electrical-to-acoustic conversion efficiency of the transducer is the same at higher intensities. The ultrasound intensities beyond the cavitation threshold were then calculated by the following equation:

$$I = \left(\frac{W}{A}\right)E \qquad [3]$$

where, W is the electrical power (measured by the wattmeter), A is the area of the transducer tip and E is the conversion efficiency (60%). Intensities used for our experiments ranged from 0.2–2.7 W/cm^2.

Electrical Resistance Measurements

The average skin conductivity was calculated as follows. The presence of skin between the donor and receiver compartments (between two electrodes) introduces an additional resistance (in series) to the already present resistance of PBS. The resistance of the skin was calculated by applying a 143 mV AC voltage at 10 Hz (Agilent 33120A, Palo Alto, CA) and measuring the current. Chamber resistance was then calculated using Ohm's law. The same procedure was repeated without mounting the skin. The difference between these two values is the resistance of the skin itself. The skin resistance was then multiplied with the skin area (1.7 cm^2) to calculate the skin resistivity. Skin conductivity is the reciprocal of skin resistivity. The skin conductivity enhancement (CE) at any time, i.e., time = t, was calculated using Eq. 4:

$$CE = \frac{C - Co}{Co} \qquad [4]$$

where, the C is the skin conductivity at time t of ultrasound application and Co is the skin conductivity before the experiment, i.e., time = 0.

Imaging of Transport Regions in the Stratum Corneum

Sulforhodamine B (Molecular Probes, Eugene, OR) was used for visualizing the transport regions in the SC. Skin was exposed to the dye along with ultrasound and/or surfactants using the methods discussed above. Skin was then removed from the diffusion cell, rinsed and was imaged using a digital camera (Optronics, Goleta, CA). Although Sulforhodamine B is a fluorescent dye it was used as a colorometric dye. The dye was used at concentrations in the range of 1 mM–5 mM. The dye was added to the donor compartment during ultrasound application to the skin. Following ultrasound application the skin was washed (after removing from the cell) to remove the dye residue on the surface of the skin, and finally imaged. The elapsed time between the removal of the skin from the diffusion cell and imaging was less than 15 min. No diffusion of sulforhodamine patches was apparent during this time.

RESULTS AND DISCUSSION

The primary objective of this study is to understand the dependence of ultrasound-induced enhancement of skin permeability on two important ultrasound parameters, that is, frequency and intensity. We have previously shown that transport enhancement induced by low-frequency ultrasound (f~20 kHz) is significantly higher than that induced by therapeutic ultrasound (f~1–3 MHz) (11). In view of this observation, we performed a detailed investigation of the dependence of permeability enhancement on frequency and intensity in the "low-frequency regime (20 kHz < f < 100 kHz)". Because a separate ultrasound transducer needs to be designed for each frequency, five discrete frequencies, 19.6 kHz, 39.6 kHz, 58.9 kHz, 76.6 kHz, and 93.4 kHz were investigated in this study. Intensity was varied over a wide range as discussed later. We have previously shown that skin conductivity is an excellent indicator of the degree of skin permeabilization due to ultrasound application, especially for hydrophilic solutes (14). Specifically, because the transdermal transport pathways used by hydrophilic solutes are similar to those used by small ions, enhancement of skin conductivity may be used as an indicator of enhancement of skin permeability. Because the measurements of skin conductivity are rapid, they were used as a measure of the effect of ultrasound on skin permeability. The precise relationship between skin conductivity and permeability depends on the size and hydrophobicity of solute. Additional studies are required to understand these relationships.

Ultrasound was applied under various frequency and intensity conditions for 15 min in the presence of 1% SLS. Figure 1 shows typical time variation of conductivity enhancement at a frequency of 36.9 kHz and six different intensities. Conductivity enhancement increased nearly linearly with time for low intensities (I < 0.96 W/cm^2). At higher intensities, a positive non-linearity was observed. We have previously shown that this type of non-linearity is prominently observed in the presence of SLS and may be attributed to the increased synergistic effect between SLS and high intensity ultrasound (13).

At any given ultrasound exposure time, the enhancement exhibited a strong dependence on intensity. For example at 36.9 kHz, no significant enhancement was observed for intensities lower than 0.54 W/cm^2 regardless of the application time (Fig. 1) (P < 0.05). On the other hand, enhancements higher than 200-fold were obtained at an intensity of 1.08 W/cm^2. A conductivity enhancement of 200-fold corresponds to a chamber conductivity of 0.565 (KOhm.cm)$^{-1}$, which is comparable to the chamber conductivity in the absence of the skin, i.e., 0.615 (KOhm.cm)$^{-1}$. This high value could be interpreted as the lack of significant skin barrier, which could potentially diminish the accuracy of comparison. For this reason conductivity enhancement values at the end of 10-min sonication will be used in further parts of the discussion for a more precise comparison.

The dependence of enhancement on ultrasound intensity

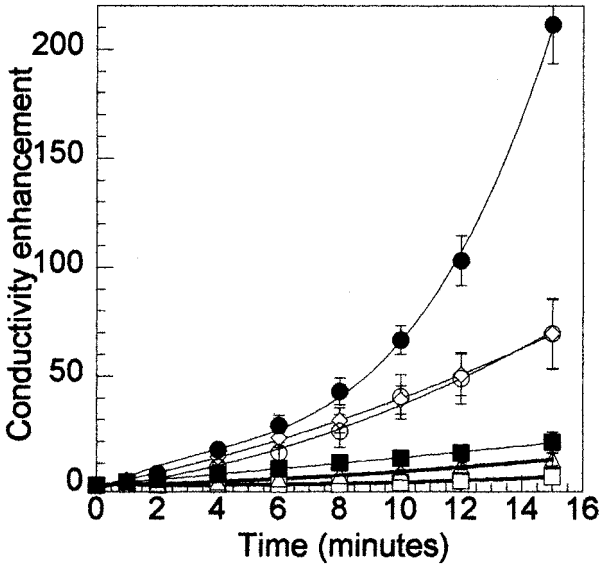

Fig. 1. The variation of skin conductivity enhancement as a function of time for 36.9 kHz at 6 different intensities ((□)-0.54 W/cm^2, (△)-0.60 W/cm^2, (■)-0.84 W/cm^2, (◇)-0.96 W/cm^2, (●)-1.08 W/cm^2, (○)-1.26 W/cm^2). The lines are presented to show the trend. Each data point represents an average of 6–8 experiments.

can be clearly seen from Fig. 2, which shows the conductivity enhancement at the end of 10-min of sonication as a function of intensity for all frequencies. For each frequency, there exists an intensity below which no detectable enhancement ($E > 1$) is observed. This intensity will be referred to as the threshold intensity. Once the intensity exceeds this threshold, the enhancement increases strongly with the intensity until another threshold intensity, referred to as decoupling intensity, is reached. Beyond this intensity, the enhancement does not increase with further increase in the intensity due to acoustic decoupling (for example, the decoupling limit for 36.9 kHz is 1.08 W/cm^2 (●), which results in decreased conductivity enhancement at higher intensities, 1.26 W/cm^2 (○), Fig. 1). This phenomenon refers to the generation of excess cavitation near the transducer, thereby reducing propagation of ultrasound to the skin (all data points in Fig. 2 correspond to intensities lower than the decoupling intensity).

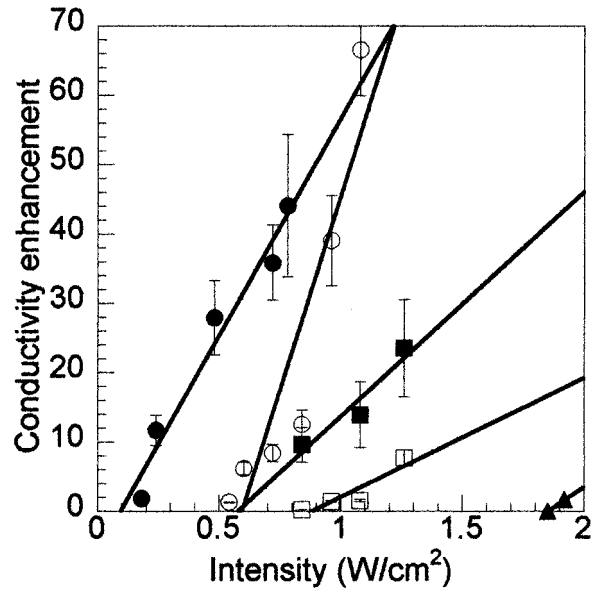

Fig. 2. The variation of skin conductivity enhancement as a function of intensity for five frequencies ((●)-19.6 kHz, (○)-36.9 kHz, (■)-58.9 kHz, (□)-76.6 kHz, (▲)-93.4 kHz). For 93.4 kHz, no additional experiments were carried out due to the limitations on the intensity of the transducer. The lines correspond to linear fits to the data (r^2 = 0.98, 0.92, 0.96, 0.91, 1.00, for 19.6 kHz, 36.9 kHz, 58.9 kHz, 76.6 kHz, and 93.4 kHz, respectively). Each point represents an average of 6–8 experiments. Threshold intensities were statistically significant ($P < 0.05$).

The relationship between conductivity enhancement and intensity is clearly different for each frequency. The threshold intensity increases from about 0.10 W/cm^2 for 19.6 kHz to 1.94 W/cm^2 for 93.4 kHz. The origin of this substantial increase in the threshold intensity may be attributed to cavitation, which plays a major role in low-frequency sonophoresis. Acoustic cavitation involves the creation and oscillation of gas bubbles in a liquid (15,16). Periodic and sustained oscillations of bubbles during alternating pressure cycles of the wave are referred as stable cavitation (15). Transient cavitation however, occurs at higher acoustic pressures and involves rapid implosion of gas bubbles after a few cycles of net growth in size. These implosions could launch high velocity acoustic microjets, which possess sufficient kinetic energy to potentially alter local skin structure. Both types of cavitation (stable and transient) depend strongly on ultrasound frequency (17). For example, number of transient cavitation events is inversely correlated with applied frequency, because at higher frequencies the time between the positive and negative portions of the acoustic cycle is too short for bubbles to exhibit a net growth in size. We have shown that the increase in the threshold intensity with increasing ultrasound frequency in Fig. 2 is consistent with the increased threshold for transient acoustic cavitation (unpublished data).

The dependence of conductivity enhancement on ultrasound frequency can be clearly seen from Fig. 3, which shows

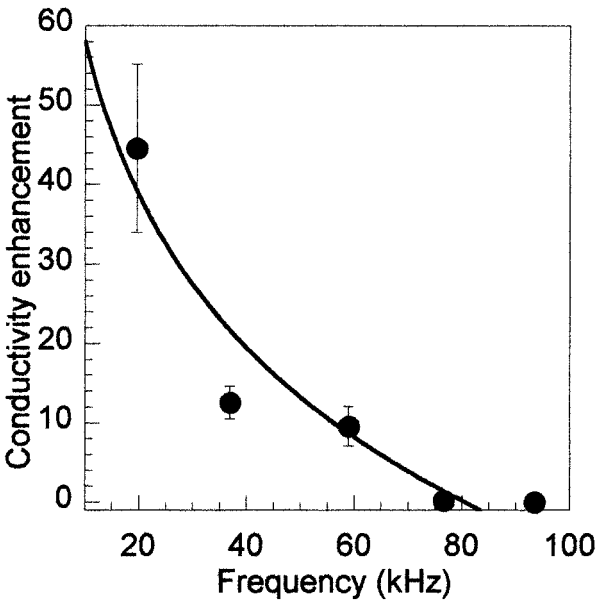

Fig. 3. The skin conductivity enhancement as a function of frequency. The curve fit shows the trend to the reader. Each point represents an average of 6–8 experiments.

enhancements at five different frequencies at a constant intensity of 0.84 W/cm^2 and a constant application time of 10 min. The enhancement decreased dramatically from about 45-fold at a frequency of 19.6 kHz to zero at a frequency of 93.4 kHz. Such a rapid decrease of permeability enhancement with ultrasound frequency is consistent with the role of cavitation in low-frequency sonophoresis, which also decreases rapidly with ultrasound frequency.

The linear dependence of conductivity enhancement on application time (in most cases, see Fig. 1) and on intensity (Fig. 2) suggests that the enhancement is likely to be a function of total ultrasound energy density (that is, a product of intensity (W/cm^2) and exposure time (seconds). In fact, we have previously shown that the enhancement induced by ultrasound at 20 kHz depends on the total ultrasound energy density (14). Specifically, no enhancement was obtained until a threshold energy density was reached beyond which the enhancement increased with increasing ultrasound energy density. We assessed whether a similar trend is also observed at other frequencies. Figure 4 shows a plot of skin conductivity enhancement against ultrasound energy density at five ultrasound frequencies (19.6 kHz, 36.9 kHz, 58.9 kHz, 76.6 kHz, and 93.4 kHz). Data for different frequencies clearly pool into separate groups, although they all follow the same general trend. Some scatter is observed in the data, which may be attributed to minor non-linearities as shown in Fig. 1.

As a general trend, no significant enhancement ($E > 1$) is observed at each frequency until a threshold energy density is reached. The threshold energy densities for various frequencies are 10 J/cm^2 for 19.6 kHz, 63 J/cm^2 at 36.9 kHz, 103 J/cm^2 at 58.9 kHz, 304 J/cm^2 for 76.6 kHz, and 1305 J/cm^2 at 93.4 kHz. Thus, the threshold energy density increased by about 130-fold as the frequency increased from 19.6 kHz to 93.4 kHz. Note that the threshold intensity increased by a factor of about 20 as the frequency increased from 19.6 kHz to 93.4 kHz. The dependence of enhancement on energy density after the threshold is different for different frequencies. For lower energy densities, the differences between various different frequencies are significant and the choice of frequency may affect the effectiveness of sonophoresis. Fundamentally, these data suggest that as the energy density increases, the differences between frequencies become less significant. For extremely high-energy densities (say 10^5 J/cm^2), the enhancement induced by all the frequencies could be comparable. (Note that high energy densities could still be achieved with intensities below the decoupling limit with longer application times). This can be seen clearly from Fig. 5, which shows a plot of the energy density required to achieve a certain enhancement (E = 1, 10, and 100) against ultrasound frequency. The lines were calculated using the power fits obtained from Fig. 4. Two observations can be made from Fig. 5. First, for any value of enhancement, there exists an energy density (regardless of frequency) that can be used to achieve that value of enhancement, although the energy density increases substantially with ultrasound frequency. Second, the ratio of the energy densities corresponding to 93.4 kHz and 19.6 kHz required to achieve the desired enhancement is higher at lower values of enhancements. It should be noted that although Figs. 4 and 5 suggest the possibility to achieve a desired conductivity enhancement regardless of the choice of frequency, due to the non-linearity of cavitation and biological systems in general, further experiments should be carried out at high energy densities to investigate this issue in detail.

A fundamental question arises whether the effect of ultrasound on skin structure is indeed insensitive to ultrasound frequency. This question cannot be answered based on the conductivity data alone as the same conductivity can be obtained via several different skin structures. For example, one large transport pathway and several small pathways may po-

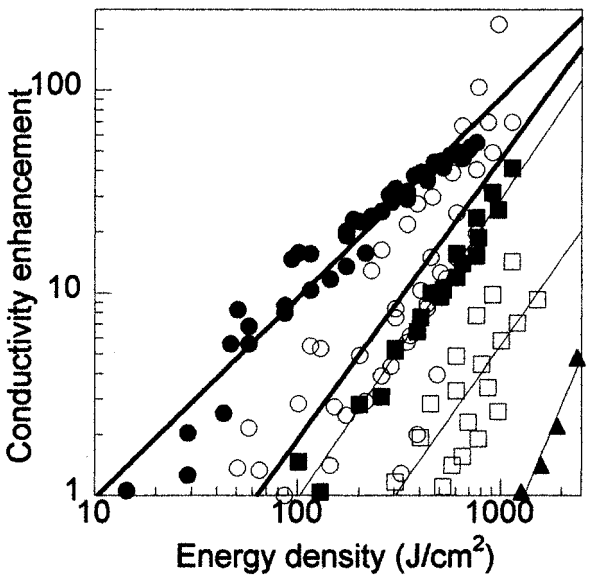

Fig. 4. The skin conductivity enhancement as a function of energy density for five frequencies ((●)-19.6 kHz, (○)-36.9 kHz, (■)-58.9 kHz, (□)-76.6 kHz, (▲)-93.4 kHz)). The lines correspond to power fits to the data (r^2 = 0.97, 0.74, 0.97, 0.71, 0.99 for 19.6 kHz, 36.9 kHz, 58.9 kHz, 76.6 kHz, and 93.4 kHz, respectively). Each point represents an average of 6–8 experiments.

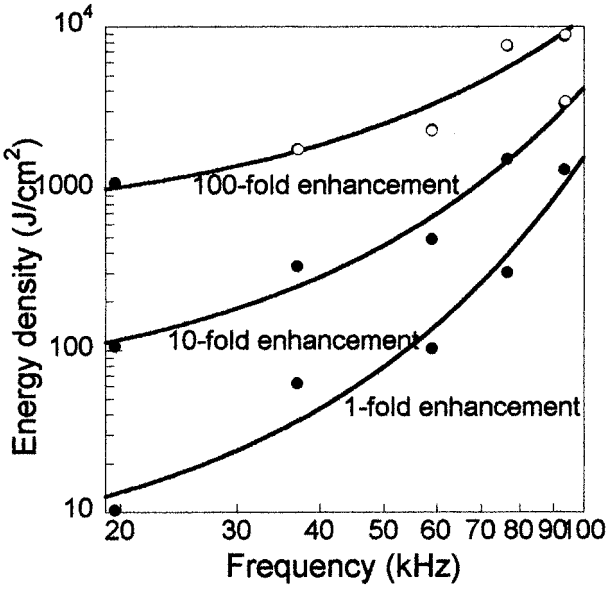

Fig. 5. Energy density as a function of frequency. Three enhancement values of 1, 10, 100-folds are presented. The lines were calculated using the power fits obtained from Fig. 4. The r^2 values for the curve fits are 0.99, 0.99, 0.95, respectively. Data points within the experimental range correspond to closed circles whereas open circles correspond to extrapolated data.

tentially result in the same conductivity enhancement. To assess this issue we performed imaging experiments. We used Sulforhodamine B (SRB), a well studied dye (18), as a model permeant.

Figure 6 shows typical images of skin exposed to ultrasound at three different frequencies at the same intensity (~0.8 W/cm^2). Application time was chosen such that the conductivity enhancement ($E \sim 30$) was the same for all samples. Despite possessing the same conductivity, the images appear very different at different frequencies. At 19.6 kHz (Fig. 6a), ultrasound appears to introduce a single, large permeability pathway in the skin. This region was intensely stained. With an increase in ultrasound frequency, the number of transport regions increased substantially. At 36.9 kHz (Fig. 6b), several distinct transport regions can be clearly seen. Even more transport regions were observed at 58.9 kHz (Fig. 6c). Similar experiments were also performed at higher frequencies (76.6 kHz and 93.4 kHz at the same intensity and application time), however, identification of transport regions was difficult since the transport enhancements induced by ultrasound under these conditions are relatively small. Additional imaging experiments were performed where application time was also fixed in addition to intensity for different frequencies (data not shown). These experiments showed that the number of transport regions still increased with increasing frequency suggesting that the differences observed in Fig. 6 could not be due to ultrasound duration but directly due to ultrasound frequency. The images in Fig. 6 conclusively show that the dispersion of transport regions increases with increasing frequencies (at constant intensity application); however, the magnitude of enhancement decreases significantly with the frequency. These two results suggest that 58.9 kHz appears to be the preferred application frequency where substantial conductivity enhancements can be obtained with reasonable energy densities while simultaneously achieving good dispersity of transport regions.

We conducted additional imaging experiments at 36.9 kHz (application time of 8 min) in the presence of SRB/SLS solution in order to study the time dependence of transport pathways. In these experiments, the skin was removed from the diffusion cells and imaged every 2 min to assess the time evolution of transport pathways. The circles in Fig. 7 indicate the area of the skin exposed to ultrasound in the presence of SRB. Figure 7 shows that the number of transport pathways increases systematically with time. This behavior is in contrast to that of 19.6 kHz, where ultrasound generates one large transport region during early moments of sonication and makes it more permeable as a function of time (Fig. 6a). Thus, while the time evolution of skin conductivity at 19.6 kHz appears to primarily originate from increasing the effectiveness of the same region, the time evolution of 36.9 kHz appears to originate from generation of new regions as well as potentially making the existing regions more permeable. Higher frequencies show the same behavior as 36.9 kHz, i.e., number of transport pathways increases systematically with time.

CONCLUSIONS

The data presented in this paper show that ultrasound in the low-frequency region is very effective in increasing skin conductivity. The conductivity enhancement increased nearly linearly with time for low ultrasound intensities. At any given exposure time, the enhancement exhibited a strong dependence on ultrasound intensity and frequency. For each frequency there exists a threshold intensity below which no detectable enhancement is observed. The threshold intensities may correspond to the lower limits of ultrasound intensity necessary to induce acoustic cavitation in the coupling medium. Due to the linear dependence of enhancement on ultrasound intensity and exposure time, the enhancement is a direct function of the total ultrasound energy density. There exists a threshold energy density below which no significant enhancement is observed. Beyond this threshold, the enhancement increases monotonically with the energy density. For lower energy densities, the enhancement-energy relationships are different for different frequencies, suggesting that the choice of frequency may affect the effectiveness of sonophoresis. However at very high energy densities, the enhancement is less sensitive to frequency. Although a given conductivity enhancement can be obtained using several ultrasound frequencies, the nature of transport pathways is different for

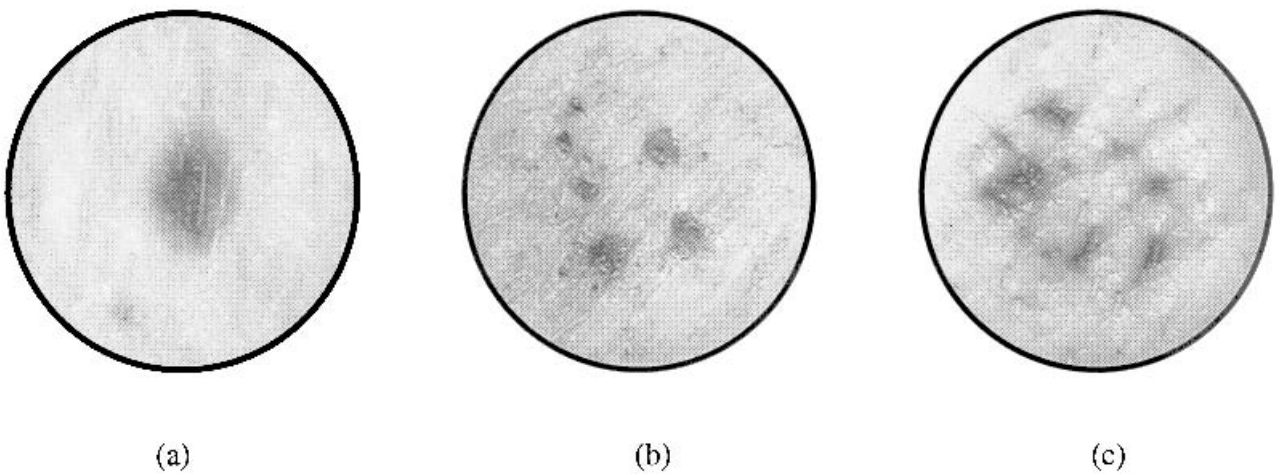

Fig. 6. Application of low-frequency ultrasound (intensity = 0.84 W/cm^2) with SLS in the presence of SRB. Potential transport regions (dark spots) are observed. (a) 19.6 kHz (application time = 6 min) (b) 36.9 kHz (application time = 9 min) (c) 58.9 kHz (application time = 14 min).

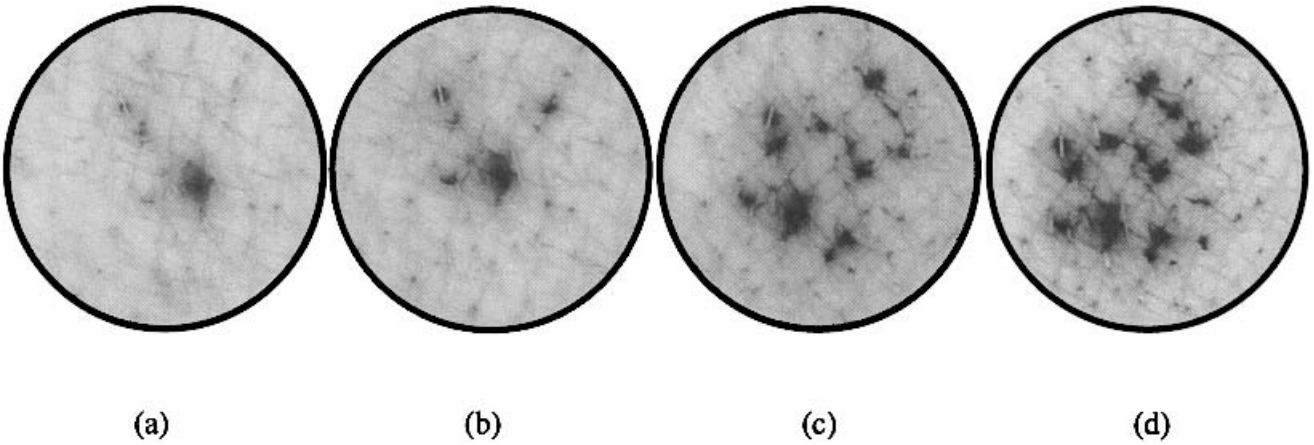

Fig. 7. Application of low-frequency (36.9 kHz) ultrasound with SLS in the presence of SRB. Images correspond to different exposure times. (a) 2 min sonication, (b) 4 min, (c) 6 min, (d) 8 min.

each frequency. At lower frequencies, ultrasound induces localized transport whereas higher frequencies generate more dispersed transport pathways.

ACKNOWLEDGMENTS

This work was supported by Centers for Disease Control and Prevention and a grant from Juvenile Diabetes Foundation. Ashley Sens acknowledges the support from the RISE fellowship from Materials Research Laboratory (MRL). Authors also acknowledge Prof. Kimberley Turner for assistance with laser interferometry.

REFERENCES

1. G. A. Simon and H. I. Maibach. The pig as an experimental animal model of percutaneous permeation in man: qualitative and quantative observations—an overview. *Skin Pharmacol. Appl. Skin Physiol.* **13**:229–234 (2000).
2. P. M. Elias. Epidermal lipids, barrier function, and desquamation. *J. Invest. Dermatol.* **80**:44–49 (1983).
3. T. M. Suhonen, J. A. Bouwstra, and A. Urtti. Chemical enhancement of percutaneous absorption in relation to stratum corneum structural alteration. *J. Control. Release* **59**:149–161 (1999).
4. B. Forslind, S. Engstrom, J. Engblom, and L. Norlen. A novel approach to the understanding of human barrier function. *J. Dermatol. Sci.* **14**:115–125 (1997).
5. K. A. Walters and J. Hadgraft. *Pharmaceutical Skin Penetration Enhancement,* 59, Marcel Dekker, New York, 1993
6. R. B. Walker and E. W. Smith. The role of percutaneous penetration enhancers. *Adv. Drug Deliv. Rev.* **18**:295–301 (1996).
7. Y. N. Kalia and R. H. Guy. Interaction between penetration enhancers and iontophoresis: Effect on human skin impedance in vivo. *J. Control. Release* **44**:33–42 (1997).
8. M. R. Prausnitz, V. Bose, R. Langer, and J. C. Weaver. Electroporation of mammalian skin: A mechanism to enhance transdermal drug delivery. *Proc. Natl. Acad. Sci.* **90**:10504–10508 (1993).
9. D. Levy, J. Kost, Y. Meshulam, and R. Langer. Effect of ultrasound on transdermal drug delivery to rats and guinea pigs. *J. Clin. Invest.* **83**:2974–2978 (1989).
10. S. Mitragotri, D. Blankschtein, and R. Langer. Transdermal drug delivery using low frequency sonophoresis. *Pharm. Res.* **13**:411–420 (1996).
11. S. Mitragotri, D. Blankschtein, and R. Langer. Ultrasound-mediated transdermal protein delivery. *Science* **269**:850–853 (1995).
12. W. Gaertner. Frequency dependence of acoustic cavitation. *J. Acoust. Soc. Am.* **26**:977–980 (1954).
13. S. Mitragotri, D. Ray, J. Farrell, H. Tang, B. Yu, J. Kost, D. Blankschtein, and R. Langer. Synergistic effect of Low-Frequency Ultrasound and Sodium Lauryl Sulfate on Transdermal Transport. *J. Pharm. Sci.* **89**:892–900 (2000).
14. S. Mitragotri, J. Farrell, H. Tang, T. Terahara, J. Kost, and R. Langer. Determination of threshold energy dose for ultrasound-induced transdermal drug transport. *J. Control. Release* **63**:41–52 (2000).
15. K. S. Suslick. *Ultrasound: Its chemical, physical, and biological effects*, VCH Publishers, New York, 1989.
16. E. A. Neppiras. Subharmonic and other low-frequency emission from bubbles in sound irradiated liquids. *J. Acoust. Soc. Am.* **46**:587–601 (1968).
17. J. Liu, T. N. Lewis, and M. R. Prausnitz. Non-invasive assessment and control of ultrasound mediated membrane permeabilization. *Pharm. Res.* **15**:918–924 (1998).
18. U. F. Pliquett, T. E. Zewert, T. Chen, R. Langer, and J. C. Weaver. Imaging of fluorescent molecule and small ion transport through human stratum corneum during high voltage pulsing: localized transport regions are involved. *Biophys. Chemist.* **58**: 185–204 (1996).